Scientia Iranica (2024) 31(5), 441–457

Sharif University of Technology
Scientia Iranica
Transactions D: Computer Science & Engineering and Electrical Engineering
https://scientiairanica.sharif.edu

Investigation of transformer vibration characteristics using the finite element method

A. Esmaeili Nezhad and M.H. Samimi*

School of Electrical and Computer Engineering, College of Engineering, University of Tehran, Tehran 1417935840, Iran.

Received 4 September 2021; received in revised form 26 December 2021; accepted 25 April 2022

KEYWORDS
Condition monitoring; Finite Element Method (FEM); Transformer winding; Vibration analysis; Vibration modes; Winding deformation.

Abstract. Understanding the vibrational characteristics of power transformers is significantly important in their design and monitoring. In this contribution, a model with a multi-physics coupling simulation of the electrical circuit, magnetic field, and solid mechanics is developed to investigate the characteristics of transformer vibration. After describing the model, the harmonic contents of the vibration signals and their variation in the case of mechanical faults are studied. It is shown that under normal operating conditions, the fundamental vibration frequency of 100 Hz has the maximum amplitude, while in the case of mechanical faults, the amplitudes of 200 Hz and 300 Hz harmonics increase dramatically compared to the fundamental harmonic. The influence of vibration sensor position is also investigated, indicating that the area near the tank bottom is the best position to gather vibration signals. Moreover, the mechanical resonance frequencies of the transformer, along with their mode shapes, are addressed in this paper. Finally, the influence of mechanical changes on the vibration energy distribution on the tank surface is explored. The results of the paper suggest possible diagnosis methods for condition monitoring of transformers, such as using the vibration energy distribution on the tank surface or analyzing the vibration harmonics.

1. Introduction

Power transformers are important components in power systems that have a major impact on the reliability of power delivery. Accordingly, various diagnostic and monitoring tools have been developed to reduce unexpected failures, although these diagnostic methods are still being developed. Referring to recent research, transformer failures can be classified as electrical, mechanical, or thermal defects [1,2]. Several diagnostic approaches for power transformers, such as dissolved gas analysis [3], partial discharge measurements [4,5], leakage reactance measurements [6], and frequency response analysis [7], have been proposed in the literature to prevent unexpected failures. The use of vibration signals to evaluate transformer health is a relatively new approach compared to other transformer condition monitoring approaches, and its research is still in its early stages. Because the vibration-based method is non-intrusive, it is an appropriate online approach.

In a large electric power system, the currents in

*. *Corresponding author. Tel.: +98 21 8801 1247*
E-mail addresses: amir.esmaeili.nej@ut.ac.ir (A. Esmaeili Nezhad); m.h.samimi@ut.ac.ir (M.H. Samimi)

To cite this article:
A. Esmaeili Nezhad and M.H. Samimi "Investigation of transformer vibration characteristics using the finite element method", *Scientia Iranica* (2024) **31**(5), pp. 441-457
DOI: 10.24200/sci.2022.59006.6012

electrical apparatuses such as transformers increase as a result of higher loading in the power transformers, which increases the electromagnetic forces produced [8,9]. Furthermore, because the electromagnetic forces are proportional to the square of the current flowing through the transformer windings, mechanical stress and mechanical oscillations on the windings are significantly increased in the event of a short circuit or inrush current [10,11]. The corresponding stresses can cause the failure of the transformer's internal structure, which is one of the most difficult problems to distinguish. Winding displacement or deformation are examples of serious problems among various mechanical failures [12]. For detecting such mechanical problems in a transformer, vibration-based monitoring systems are proposed in the literature.

Vibration-based condition monitoring refers to the use of non-destructive sensing and analysis of system characteristics in the time, frequency, or modal domains to detect changes that may indicate damage or degradation [13–18]. In recent years, researchers have conducted research on the recognition of transformer vibrational properties. In [19], Fahnoe conducted a study of the vibrational harmonics generated by the transformer core under magnetostriction. In this study, a large number of modes in which the core of various structures may vibrate were determined experimentally and analytically. In [20], a numerical study of membrane vibration properties in transformer oil was performed. This study showed that mechanical energy is transformed into thermal energy during vibration and that its amplitude continuously decreases with time. In [21], Foster and Reiplinger employed simulation techniques to investigate the impact of material and processing on vibration properties and the vibration frequency spectrum of a power transformer. Researchers in [22–25] developed mathematical models of the electromagnetic vibration of the power transformer core by coupling electromagnetic-field theory with structural mechanics theory. The magnetostriction of silicon steel sheets was simulated using these models. In [26], Ji et al. explored in detail the connection between the vibration of the winding and the iron core, developing a technique for obtaining the features of the transformer's vibration signal using wavelet analysis. In [27], Yu et al. investigated the connection between the tightening force and the natural frequency of the windings using modeling and testing. This study determined that winding pretension can influence the natural frequencies and vibration modes.

In recent years, researchers have also paid more attention to vibration-based techniques for detecting the condition of transformer windings, which can be divided into signal-based and model-based methods. Signal-based methods typically extract information from vibration signals. Researchers in [28–30] have developed a set of indicators to evaluate the condition of transformers using vibration signals. In these studies, faulty transformers show an increase in vibrational harmonics compared to healthy transformers. The use of model-based methods is the second approach to vibration diagnostic methods. For example, mathematical models were used to detect the mechanical condition of the winding in [31–33]. These studies use transformer parameters such as electric current, voltage, and temperature as model inputs.

In most studied research, the methods used were based on analytical models and experimental data. The most significant gap in these studies is that they emphasize only certain vibrational features and are unable to present comprehensive information about the transformer's vibration mechanisms. To obtain a precision plan and reach proper results, a robust method is needed, which considers the linear and non-linear characteristics of the transformer core and winding in terms of electromagnetic and mechanical features. Accordingly, the Finite Element Method (FEM) is an alternative technique for performing structural dynamic and electromagnetic field analysis because it provides precise insight into how the various elements of a design interact [34,35]. According to the aforementioned points, the motivation behind this paper is to provide a vibration-based method with regard to experimental test limitations. Because experimental tests are destructive to transformer windings, this paper uses a multi-physics coupled simulation to find a solution for diagnosing three types of winding defects named LV winding free buckling, winding elongation, and winding twisting. Accordingly, the main contributions of the paper can be summarized as follows:

- Developing a numerical model for the vibration analysis of a transformer, which can involve accurate modeling of complex structures such as core and winding assemblies. In past papers, these modeling considerations are not applied to models simultaneously;
- Employing the FEM to analyze and study the problem of the paper, which uses a multi-physics coupled simulation of the electrical circuit, magnetic field, and solid mechanics to simulate the characteristics of transformer vibration;
- Investigating the Frequency Response Function (FRF) of the transformer structure vibration using vibration modal simulation, which extends transformer modal analysis to a new level;
- Presenting a useful framework to analyze the response of transformer vibration under various operating conditions and adopt them for vibration

behavior extraction, which can be directly applied to transformer condition monitoring;

- Providing an analysis framework of the natural frequencies of the winding-related modes in the presence of winding damages as well as extracting the pattern of vibration energy distribution on the transformer tank, which has the potential to be used for the mechanical monitoring of transformers. In past research, the energy distribution patterns have not been analyzed.

The rest of the paper is structured as follows: Section 2 studies the calculation of electromagnetic forces of winding. Section 3 presents transformer modeling considerations in modeling the active part and the tank. Section 4 describes a multi-physics coupling simulation of the circuit, magnetic field, and solid mechanics. Section 5 discusses vibration spectrum analysis, including the influence of sensor positions on the tank, and compares vibration harmonics under winding mechanical faults. Afterward, Section 6 explores the mechanical resonance frequency and their corresponding mode shapes. Moreover, the effect of a possible mechanical change on the vibration energy distribution is addressed in this section. Finally, Section 7 concludes this paper.

2. Theoretical background

Transformer vibration has two main constituents: (i) winding vibration caused by the electromagnetic force generated by the interaction of the current in a winding with leakage flux, and (ii) iron core vibration caused by the magnetostriction forces in the silicon steel sheets [36,37]. In addition to the vibrations generated by the core and the windings, other components also vibrate during the operation of the transformer. Each tap changer operation produces a specific vibration wave that propagates through the oil and the structure of the transformer. Vibration analysis is usually based on periodic oscillations and does not account for tap changer vibrations, which appear only after a tap operation and produce temporary vibrations. Furthermore, experimental results show that the main components of tap changer vibrations have a frequency of a few kHz, and the large difference in frequency amplitude between the vibrations generated by the core and windings justifies analyzing them separately. The cooling system (oil pumps and fans) also generates vibrations that are added to the main vibrations produced by the core and the windings. These components do not work continuously, because they turn on or off depending on the operating temperature of the transformer, but a periodic vibration signal appears during their operation. In general, vibrations in the core/winding occur at a variety of frequencies up to several hundred Hz. These frequencies appear as even, odd, and rational multiples of the fundamental frequency, with 100 Hz and its integer multiples being the most dominant components. Vibrations also are highly correlated with transformer loads, with the 100 Hz, 200 Hz, and 300 Hz components being the most sensitive [38,39]. Vibrations with a frequency less than 100 Hz are usually produced by cooling systems and the operation of oil pumps [1,40].

By putting aside the vibrations of the cooling system and the tap-changer, two vibration sources remain: the core and the winding. Moreover, the vibration of the winding is significantly larger than the vibration of the core under both normal operating and short circuit conditions. As a result, it can be inferred that the observed vibration signals mainly comprise the winding vibration signals. The current flowing through the transformer winding can be expressed as follows:

$$i(t)=I\cos\omega t. \tag{1}$$

In Eq. (1), ω is the angular frequency, and I denotes the current amplitude. The leakage magnetic flux around the transformer winding is a function of current and changes with time. When the winding is dislocated, the distribution of the leakage magnetic flux around it also changes. Magnetic flux density (B) can be described as [41,42]:

$$B(t) = \frac{u_0}{4\pi} i(t) \int_l \frac{dl \times \hat{r}}{r^2}, \tag{2}$$

where r is the radius and dl is the infinitesimal elements of winding. Except for $i(t)$, all values at a given place in space are constant. As a result, $B(t)$ can be simplified as follows:

$$B(t) = kI\cos\omega t, \tag{3}$$

where k is the proportionality constant between I and B, and I is the current amplitude. The axial leakage flux density B_a interacts with the current passing from the windings to produce a radial force F_r. Additionally, the interaction between the current and radial component of the leakage flux B_r generates the axial force F_a. Then, using Eq. (4), the electromagnetic forces in the radial and axial directions can be defined as follows [41]:

$$F_r = i(t)B_a(t)2\pi R, \qquad F_a = i(t)B_r(t)2\pi R, \tag{4}$$

$$F = \sqrt{{F_r}^2 + {F_a}^2} = 2\pi RkI^2 \left(\frac{1}{2} + \frac{1}{2}\cos 2\omega t\right). \tag{5}$$

These calculated forces are then utilized as an excitation source for calculating the vibrations in the transformer structure. After describing the model in Section 3, the rest of the relevant equations are given in Sections 4.1 and 4.2.

3. Model description

In this study, a single-phase transformer with a disc-type winding configuration similar to a large power transformer is considered for the modeling to simplify the electromagnetic loading conditions applied to the model. It is expected that simulating a three-phase transformer does not discredit the validity of the vibration model presented in this study, provided that the model loading conditions are appropriately determined.

3.1. Modeling of the active part

Because the transformer construction is a complicated system with many different components, only those that affect the vibration response are modeled in this study. Figure 1 describes the transformer's three-dimensional (3D) FEM model. Tables 1 and 2 introduce the model's parameters, such as the geometric, electrical, and mechanical properties of the transformer components.

In practical transformers, windings are frequently made up of continuously transposed copper strands to transmit current with low eddy current losses. This design satisfies the electrical requirements, but it makes vibration modeling more difficult. To reduce the time it takes to solve the FEM model, the winding structures must be replaced with a simpler homogenized 3D model with the same form and dimension. The next challenge in the simulation is the layered core of the transformer. The meshing becomes very dense in the core due to its layered nature, and, therefore, the model needs a high computational power to be solved. In transformer vibration modeling, how to deal with this challenge is crucial. An analogous methodology based on the Young's modulus of the transformer core structure is offered to overcome this problem. Young's modulus is a mechanical property that measures the tensile stiffness of a solid material. To clarify this concept, a test specimen is made of SiFe sheets, as shown in Figure 2. The specimen is made of 100 layers of SiFe sheets with a thickness of 0.3 mm. A bolt hole is bored at each end of the SiFe sheet to clamp the laminations once

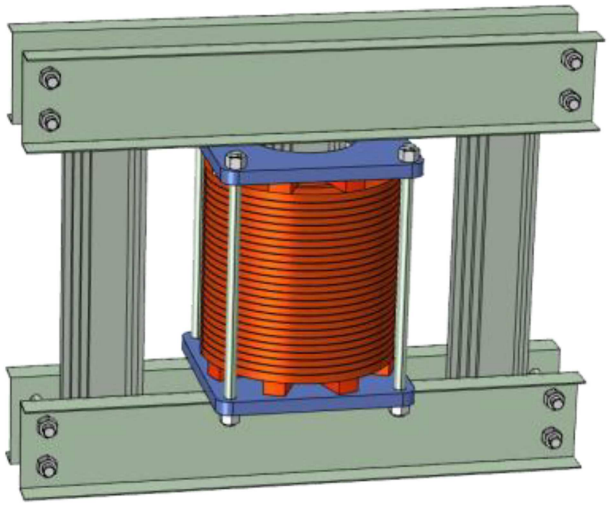

Figure 1. Transformer model for vibration analysis.

Table 1. Specifications of the test transformer.

Main technical indicators	Parameter
Phase number	Single-phase
Frequency	50 Hz
Rated power	6.3 MVA
HV rated voltage	10.5 kV
LV rated voltage	710 V
Model height (cm)	100.4
Outer/inner diameter of LV winding (mm)	200/146
Outer/inner diameter of HV winding (mm)	285/215

Table 2. Mechanical specifications of transformer components.

Component	Material	Density (kg/m^3)	Young's modulus (GPa)	Poisson ratio
Windings	Copper	8900	115	0.35
Core	SiFe	7650	180	0.25
Clamping plate	PBT	900	7.69	0.48
Bolts	Steel	7850	210	0.3
Brace	Steel	7850	210	0.3

Table 3. Test results for the in-plane and out-of-plane direction vibrations.

ID	Natural frequency (Hz)	Young's modulus (GPa)
In-plane vibration	2562	174.5
Out-of-plane vibration	135	1.9

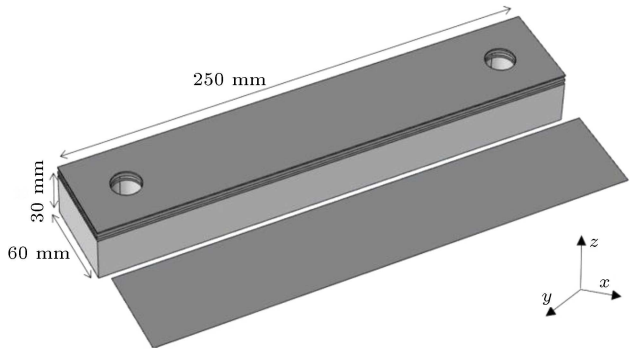

Figure 2. Test specimen laminated by SiFe sheets.

assembled. According to the Euler-Bernoulli beam theory, a simulation is carried out to determine the natural frequencies and, hence, Young's modulus. The natural frequency can be calculated analytically as follows [43]:

$$\omega_n = (\beta_n L)^2 \sqrt{\frac{EI}{\rho A_0 L^4}}, \tag{6}$$

where ω_n is the natural frequency, E is the elastic modulus, $\beta_n L$ is a constant relating to each natural frequency, A_0 is the area of the cross-section, ρ is the material density, L is the length of the core laminate, and I is the area moment of inertia.

The anisotropic Young's modulus of the test specimen is determined by measuring the vibration in both the in-plane and out-of-plane directions independently. The out-of-plane direction is along the z-axis in Figure 2. The results of the input mobility test for in-plane and out-of-plane vibrations are reported in Table 3. Two resonance frequencies of 2562 Hz and 5388 Hz are detected in the in-plane testing findings. The calculated mode shapes at the first resonance frequency always agree well with the characteristics of SiFe sheets. Eq. (6) calculates the test specimen modulus of elasticity to be $E = 174.5$ GPa, while SiFe has an elastic modulus of around 180 GPa, which is close to the estimated elastic modulus in the in-plane direction. This means that the SiFe sheet's lamination has little effect on material characteristics in the in-plane direction, and the core lamination can be considered as a solid body. Compared to the in-plane direction, the natural frequencies in the out-of-plane direction are significantly lower. This means that the vibrational properties of the core are very anisotropic. However, in practice, the core stiffness is controlled not only by the elastic modulus of the SiFe core but also by the clamping forces of the core holding structure. By considering the clamping structure, the solid body shows behavior similar to that of the layered core. Based on the aforementioned points, the core is modeled as a solid body with a varying Young's modulus along different axes.

3.2. Modeling of the tank

There are various reasons for modeling the transformer tank. The most important reason is the need to detect instances in which vibrations propagating from the active part excite a natural frequency of the tank construction. There are two ways in which the mechanical vibrations of the transformer winding can be transmitted to the tank wall [44,45]:

- Direct transfer through mechanical connections: A direct coupling between the tank and the active part is achieved through mechanical connections, with transmission taking place via the tank base, where the active part is located;
- Indirect transfer through the insulating fluid: The fluid-structure interaction provides an indirect link between the insulating fluid and the tank structure, allowing vibration waves generated by the active part to reach the tank structure.

The vibration analysis technique can diagnose internal defects in transformers because the mechanical features of the windings affect the tank vibration response. Therefore, by measuring the vibration signals from the surface of the transformer tank, the mechanical health condition of the windings can be analyzed. The tank structure model is illustrated in Figure 3. Also, a summary of the steps taken to utilize the FEM model to predict the vibration characteristics of a transformer is presented in Figure 4.

4. Multi-physics model for transformer vibration

4.1. Electromagnetic field model

To calculate electric and magnetic fields, the primary winding is connected to a 50 Hz alternating source, while the secondary winding is short-circuited. The electric field equation can be defined as follows [42,46]:

$$-\nabla.\frac{\partial(\varepsilon_0 \varepsilon_r \nabla V)}{\partial t} - \nabla.(\sigma \nabla V - J_e) = 0, \tag{7}$$

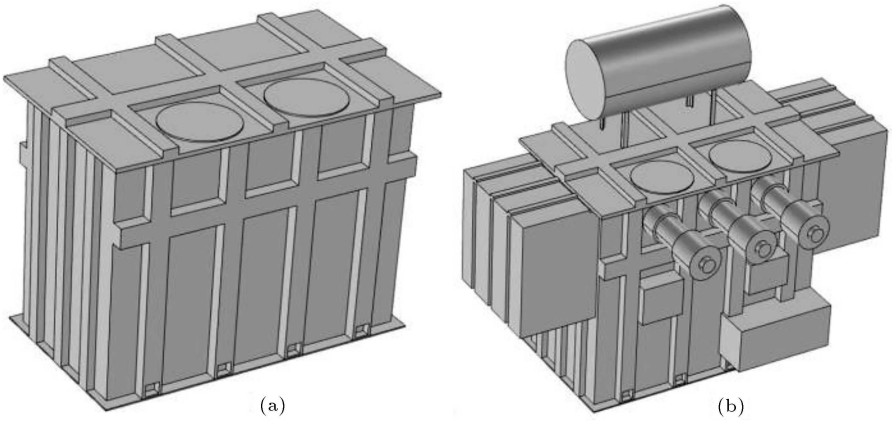

Figure 3. Finite element model of (a) the transformer tank and (b) the transformer tank with auxiliary equipment.

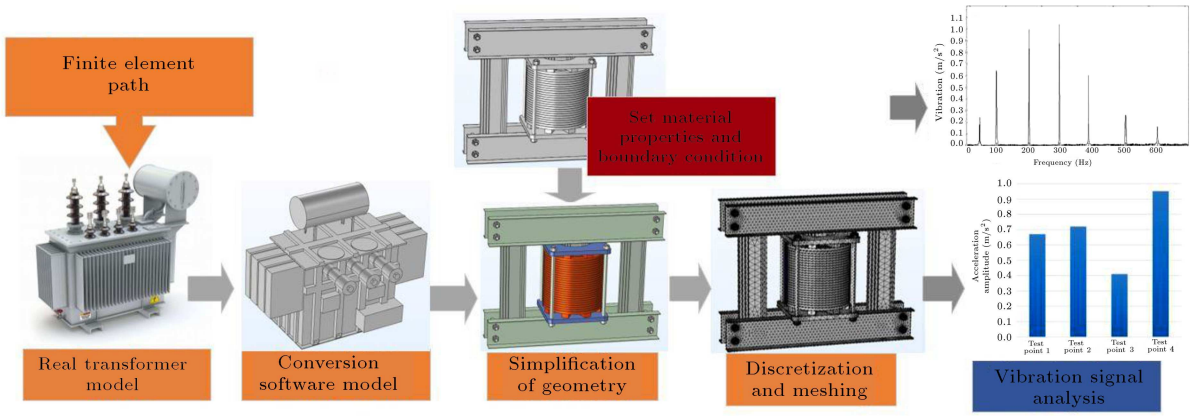

Figure 4. Steps in utilizing the finite element tool to predict the vibration response of the transformer.

where ε_0 is the dielectric constant in free space and equals 8.85×10^{-12} F/m, ε_r is the relative dielectric constant, σ is the conductivity, J_e is the external current density, and V is the potential. The current density J_e is then incorporated into the magnetic-field differential equation as follows [46]:

$$\sigma \frac{\partial A}{\partial t} + \nabla \times ({\mu_0}^{-1} {\mu_r}^{-1} \nabla \times A) = J_e, \tag{8}$$

where μ_0 is the permeability in free space and its value is $4\pi \times 10^{-7}$ H/m, μ_r is the relative permeability, and A is the magnetic vector potential. In addition, the magnetic field's governing equation is as follows [47]:

$$B = \mu_0 \mu_r H = \nabla \times A, \tag{9}$$

$$J = \sigma E + J_e, \tag{10}$$

where B, H, and E represent the magnetic flux density, the magnetic field, and the electric field, respectively. The meshes were built using adaptive refinement methods, thus they are substantially finer in areas of high variation and strength of the magnetic field, as shown in Figure 5. Figure 6 shows mesh quality, and where a value closer to 1 indicates higher mesh quality. Figure 7(a) and (b) shows the results of the magnetic model at the point where the current going through the winding reaches 70% of its peak value. At this time, the highest B in the winding area is 0.06 T, whereas the maximum B in the core is 1.6 T. The simulation findings are consistent with the specifications of single-phase transformers, implicitly indicating the correctness of the model. Now, the model can be developed to simulate the vibration analysis, as will be discussed in the next subsection.

4.2. Mechanical vibration model

Winding vibration is influenced by the mass inertia, elasticity, and damping of the winding. The differential equations of motion for solid mechanics are given in Eq. (11) [46,48]:

$$M_i \frac{d^2 z}{dt^2} + C_i \frac{dz}{dt} + K_i z = f(t), \tag{11}$$

where M_i denotes the mass matrix, C_i denotes the damping coefficient matrix, K_i denotes the stiffness coefficient matrix, z denotes the winding's deformation (displacement), the first derivative of z indicates the winding's deformation velocity, the second derivative of

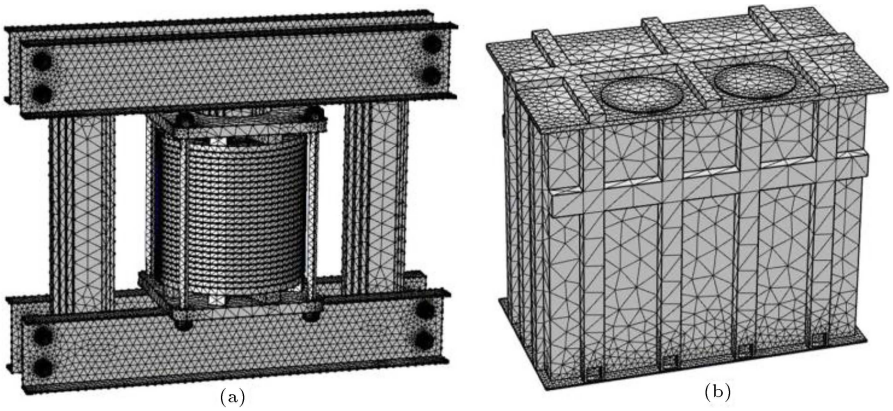

Figure 5. Mesh-generation results for (a) transformer 3D geometric model and (b) transformer tank.

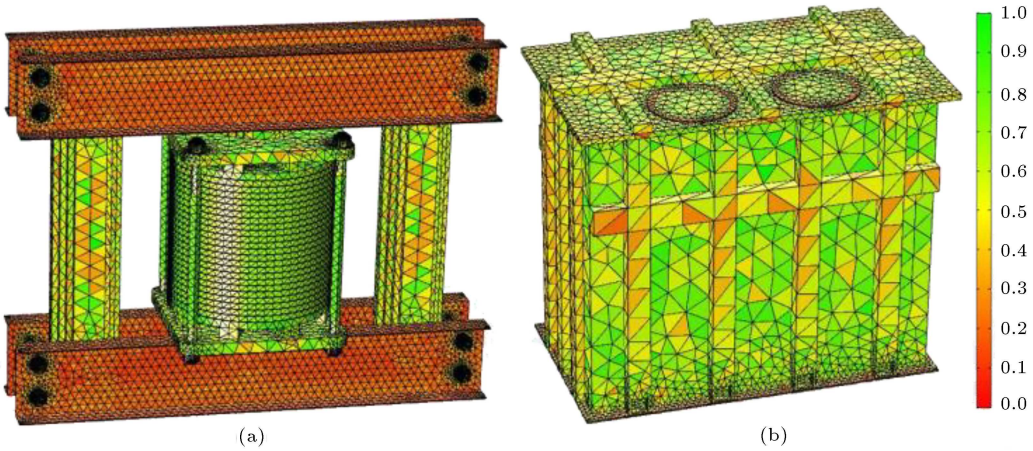

Figure 6. Quality diagram of mesh grid division for (a) transformer model and (b) transformer tank.

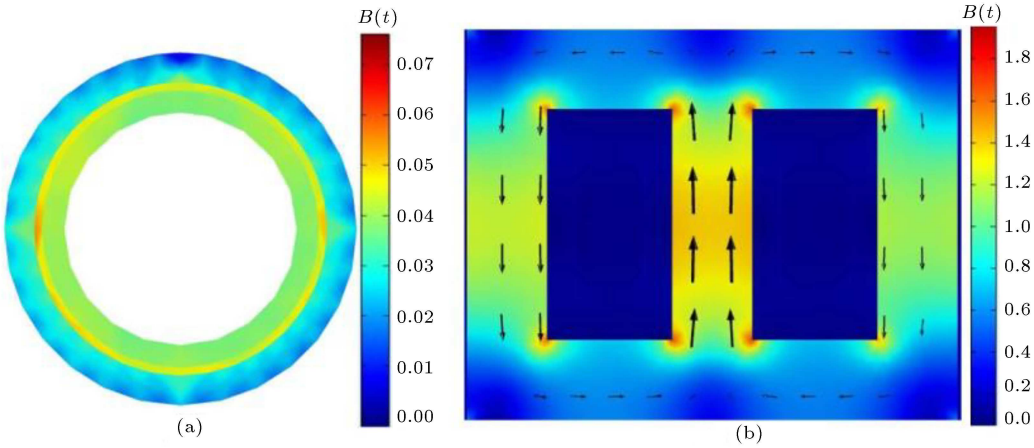

Figure 7. Distribution of magnetic flux density in the (a) winding and (b) core.

z denotes the winding's deformation acceleration, and $f(t)$ denotes the force magnitude. The displacement equation of the transformer winding can be calculated by adding Eq. (5) into Eq. (11) [41,46]:

$$z(t) = Ye^{-\frac{C_i t}{2M_i}}\sin(\omega_0 t+\theta) + G\cos(2\omega t+\varphi), \qquad (12)$$

in which:

$$G = \frac{BI^2}{\sqrt{(K_i - 4M_i\omega^2)^2 + 4{C_i}^2\omega^2}},$$

$$\tan\varphi = -\frac{2C_i\omega}{K_i - 4M_i\omega^2}.$$

In Eq. (12), Y and θ are set by the initial conditions, ω and ω_0 are the current angular frequency and the

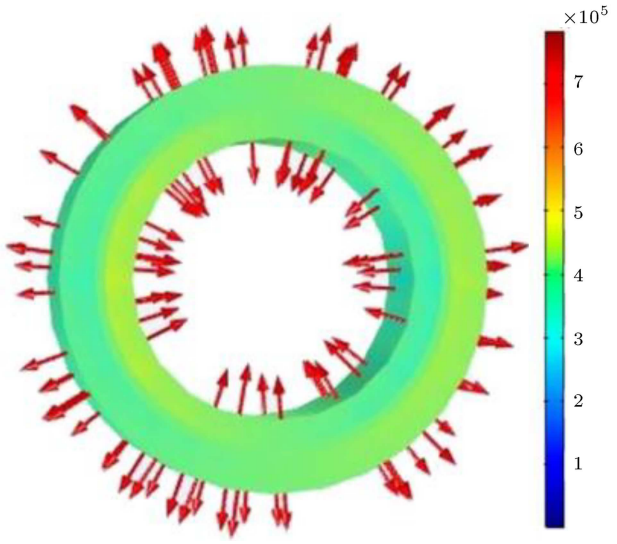

Figure 8. Distribution diagram of the radial stress (N/m^3) in the transformer winding.

natural oscillation frequency of the transformer winding, I is the current amplitude, and B is the magnetic flux density. The acceleration of the winding vibrations according to Eq. (13) can now be calculated using the second derivative of Eq. (12) [41]:

$$a = -\omega_0^2 Y e^{-\frac{C_i t}{2M_i}} \sin(\omega_0 t + \theta) - 4\omega^2 G \sin(2\omega t + \varphi). \quad (13)$$

Furthermore, for the solution to converge, the fixed boundary condition is applied at both ends of the winding. It is noteworthy that both winding ends are clamped by press rings and, therefore, the fixed boundary condition is a suitable choice.

Figure 8 shows an output result of the multi-physics model, illustrating the radial forces on the transformer. The radial forces of the windings, as shown in Figure 8, cause mechanical stress on the high-voltage winding in the outward direction, while the internal low-voltage winding is compressed inwards. These results are consistent with the expected behavior of the winding. This indicates the model functionality in investigating the mechanical structure of the transformer with electrical inputs.

5. Analysis of transformer vibration signals

In this section, the vibration signals of the winding are measured from the aforementioned model and analyzed. To guarantee that the location of the tank where the vibrations are measured appropriately represents the transformer's internal behavior, the first step is to evaluate a correlation between several measurement points on the tank wall and the resulting acceleration signals. Then the spectrum of vibration signals in different operating conditions is studied as a criterion for determining the mechanical condition of the winding.

5.1. Influence of sensor positions

First, the correlation between various measurement locations on the tank wall and the resulting vibration signals is investigated. Figure 9(a) depicts the transformer tank with 5 measurement points. These test points are located in the mid-height of the tank. To capture the vibration signals, the acceleration is measured at each test point, similar to most practical vibration sensors. Figure 9(b) depicts the observed vibration harmonics at the tank center point (test point 3). As can be observed, higher vibration harmonics have a smaller amplitude than the 100 Hz component. Because of the high signal power of 100 Hz, this vibration component is considered the vibration fundamental frequency. Therefore, it is used in other subsequent analyses of the transformer vibration signals.

Figure 10 depicts the vibrations observed at 5 test locations at the vibration fundamental frequency (100 Hz). The results show that the signal amplitude is higher at the edges of the transformer tank (at test

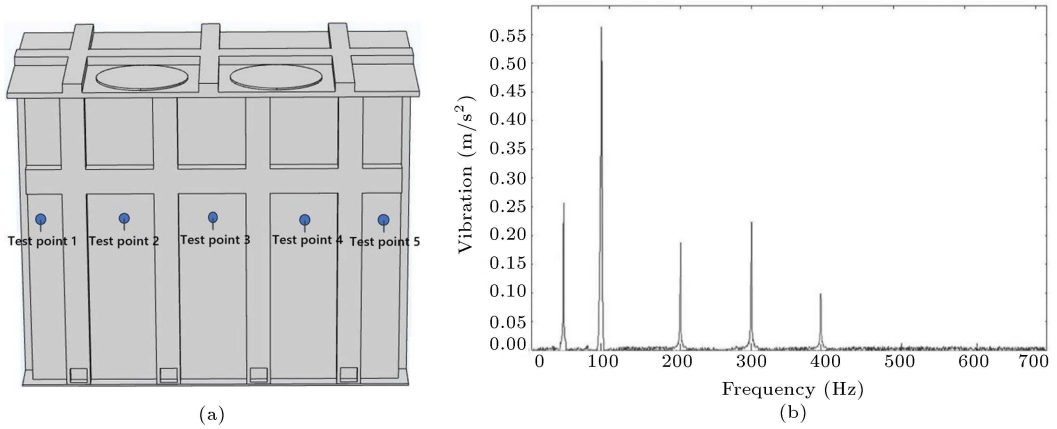

Figure 9. (a) Locations of measurement points on the transformer tank wall: (b) Vibration harmonic spectrum measured at test point 3.

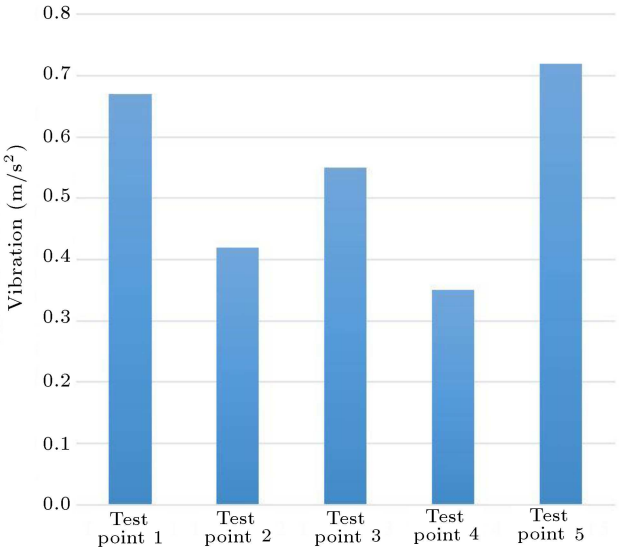

Figure 10. Fundamental frequency (100 Hz) amplitude of the vibration at different test point locations, compare positions to Figure 9.

points 1 and 5). This indicates that the use of vibration to assess transformer condition is highly dependent on sensor positions. In other words, the mechanical changes are measurable at any measurement position, but they are not comparable to each other. These results are consistent with the results obtained from laboratory experiments performed on a real power transformer [49].

Because the amplitude of the vibration signals measured from the transformer tank varies at different measuring locations, an additional test is carried out to find the optimal zone for vibration signal measurement. Figure 11(a) depicts the position of the measuring locations on the tank surface. The vibration measured at point 4 near the tank bottom shows the highest power of the detected vibration signals, as illustrated in Figure 11(b). Based on the results of these tests, it can be concluded that the best location to measure the mechanical oscillations on a transformer is near the tank bottom. These results are consistent with those based on laboratory studies on large real power transformers in [32,41,50,51]. This can also indicate the accuracy of the proposed finite element model in monitoring transformer vibration signals, which can be used for further vibration signal analysis.

5.2. *Transformer vibration analysis under winding mechanical faults*

Analyzing the vibration features of transformer windings reveals that as the mechanical condition of the windings varies, so does the corresponding mechanical vibration. According to [28,30,33], the fundamental frequency component consists of vibration signals of the windings, while the high-frequency vibrations of the tank surface are mainly caused by magnetostriction of the core and are independent of winding vibration. Therefore, the low-frequency vibrations measured on the tank surface can be used to diagnose the condition of the windings directly. Moreover, according to [52], when the relative value of the transformer vibrational harmonic magnitude changes significantly, the windings are deemed to have a serious fault, and the transformer must be taken out of operation. This point is demonstrated in this section using the proposed model as well. In this section, the multi-physics model is used to detect three types of winding defects: LV winding free buckling, winding elongation, and winding twisting, as shown in Figure 12.

Figure 13 shows a spectrum-analysis diagram of the vibration signals at a measurement point near the tank bottom under healthy winding conditions and when winding mechanical changes occur. As depicted in Figure 13(a), under normal operating conditions, the

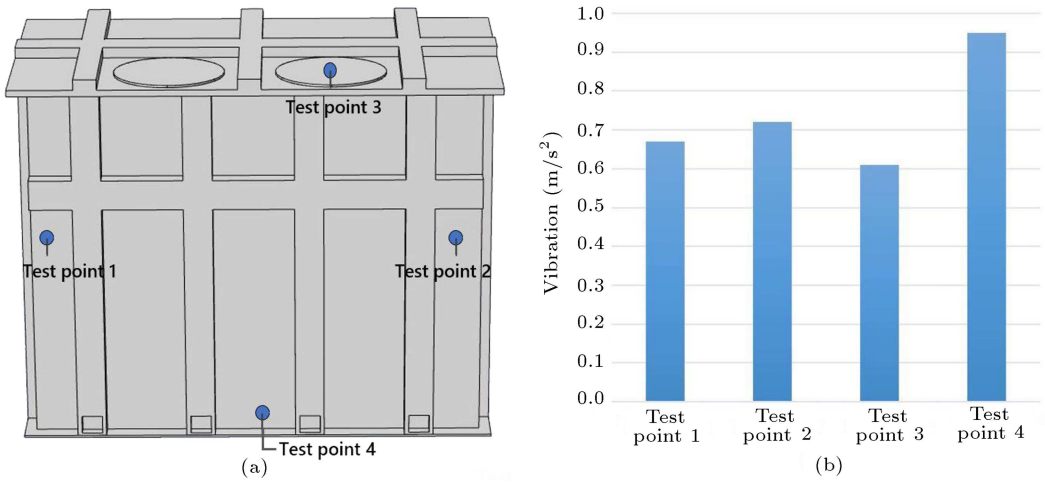

Figure 11. (a) Measurement points on the test transformer tank; (b) Fundamental frequency (100 Hz) amplitude of the vibration at different test point locations.

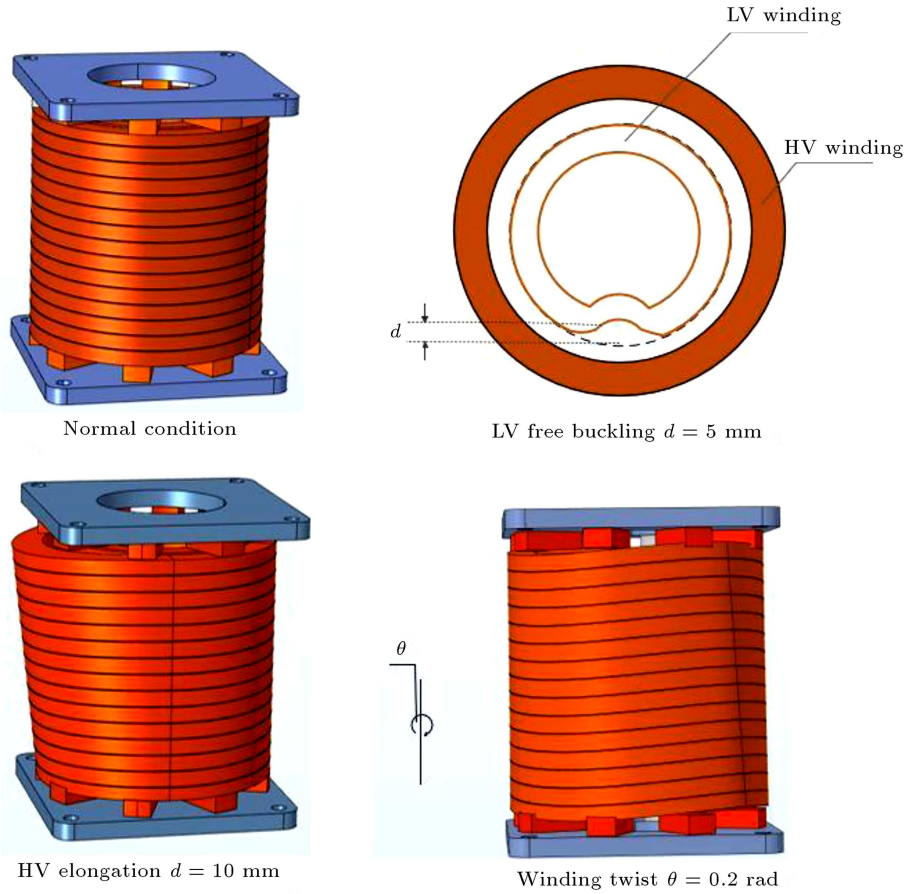

Figure 12. Schematics of types of winding damage.

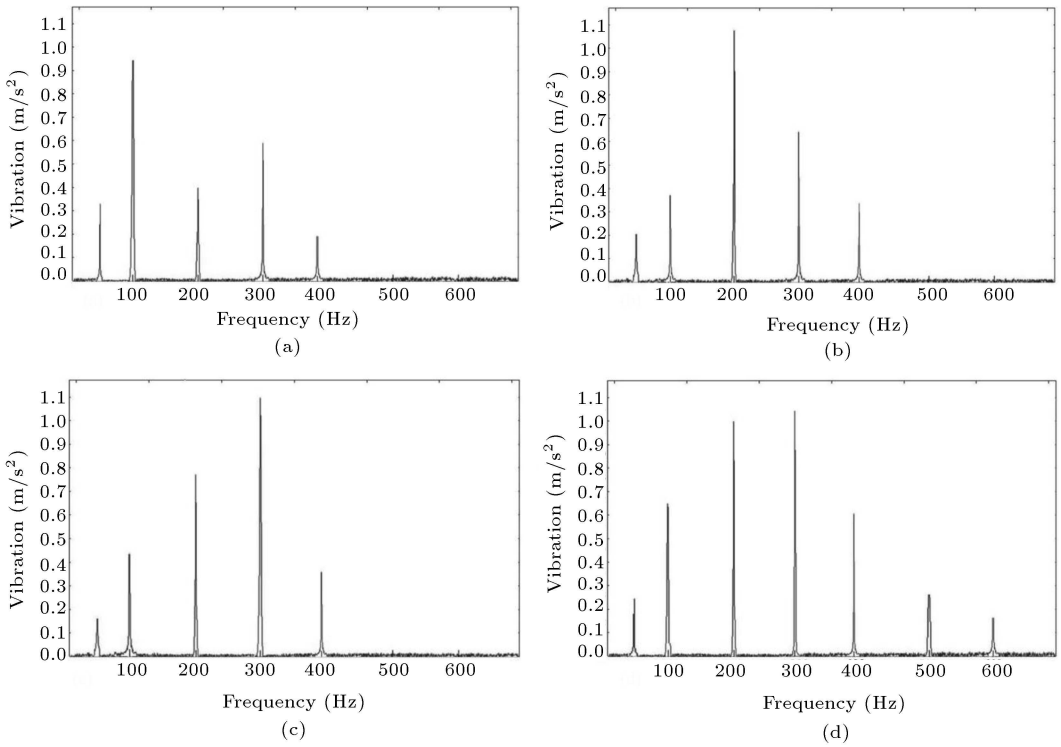

Figure 13. Vibration spectrum measured at pint 4 under different operating conditions: (a) normal condition; (b) LV free buckling; (c) HV elongation; and (d) winding twisting.

Table 4. The amplitudes of vibration harmonics in different cases of Figure 13 in m/s^2 (NS declares not significant).

Cases	Frequency of the Harmonic						
	50 Hz	**100 Hz**	**200 Hz**	**300 Hz**	**400 Hz**	**500 Hz**	**600 Hz**
Normal condition	0.33	0.95	0.40	0.59	0.19	NS	NS
LV free buckling	0.20	0.37	1.08	0.64	0.33	NS	NS
HV elongation	0.17	0.43	0.77	1.09	0.36	NS	NS
Winding twisting	0.24	0.65	1.01	1.05	0.61	0.27	0.16

maximum amplitude of vibration signals is obtained at the vibration fundamental frequency of 100 Hz (0.95 m/s^2). Other vibrating harmonics with frequencies of 50 Hz (0.33 m/s^2), 200 Hz (0.4 m/s^2), 300 Hz (0.59 m/s^2), and 400 Hz (0.19 m/s^2) with amplitudes less than 100 Hz are also seen in this diagram, indicating the healthy mechanical condition of the winding. In the presence of mechanical faults in the winding, as shown in Figure 13(b)–(d), the amplitudes of the 200 Hz and 300 Hz harmonics increase dramatically compared to 100 Hz. When a buckling fault occurs for the winding, the maximum harmonic amplitude occurs at 200 Hz (1.08 m/s^2), and the 300 Hz (0.64 m/s^2) harmonic exhibits higher amplitudes than the fundamental frequency (0.37 m/s^2). In the case of the winding elongation fault, the 300 Hz (1.09 m/s^2) harmonic has a maximum amplitude, and the 200 Hz (0.77 m/s^2) harmonic has an amplitude greater than the fundamental frequency (0.43 m/s^2). In the case of the winding twisting fault, other vibrating harmonics, including 500 Hz (0.27 m/s^2) and 600 Hz (0.16 m/s^2), appear in the vibration spectrum. As shown in Figure 13(d), in this case, the 300 Hz (1.05 m/s^2) and 200 Hz (1.01 m/s^2) harmonics also have amplitudes greater than the fundamental frequency (0.65 m/s^2). Table 4 presents the amplitudes of all harmonics in these four cases. According to these results, it is reasonable to conclude that when the amplitude of other harmonics is greater than the amplitude of the main vibration frequency (100 Hz) in the vibration frequency spectrum, the transformer winding may have a serious mechanical fault. Moreover, the presence of higher-order vibration harmonics in the vibration frequency spectrum, such as 500 Hz and 600 Hz, may indicate mechanical twisting in the winding. This study shows that analyzing the vibration harmonics and their amplitudes (ratios) during transformer operation has the potential to detect mechanical changes in the winding.

6. Analysis of transformer vibration modes

The introduced FEM model can also serve for further studies on transformer vibration. In this section, the model is used to investigate the vibration frequency response of the transformer. Through frequency response analysis, different modes and resonances can be distinguished, and it is also possible to correlate each vibration mode with specific sections of the transformer. Moreover, utilizing the provided model, this section demonstrates that mechanical changes within the transformer affect these modes and, therefore, can be used as a diagnostic tool.

6.1. Dynamic analysis of the transformer structure

Figure 14 illustrates the average FRF of the transformer vibration. The resonant behavior of the transformer structure is visible in the frequency ranges, where the response amplitude gradually increases with increasing frequency. This means that vibrations are more easily excited by an input force at higher frequencies. Because of the sensitivity of the human ear, restrictions on noise output at higher frequencies are crucial. Therefore, transformer designers need to optimize their designs to reduce high-frequency components. Furthermore, the number of resonant peaks in the low-frequency range, particularly in the operating frequency range (50 Hz and its harmonics), is greater than those in the high-frequency range. This necessitates the optimal design of transformers to weaken resonant modes in the low-frequency range.

The suggested model can also identify which elements are involved in each resonance mode. For this purpose, each resonance should be excited to realize which elements are active in that mode. This feature has been implemented for all resonance points, and the results of the first thirteen natural frequencies are

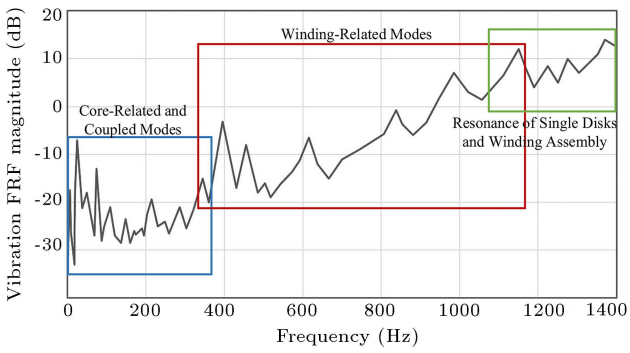

Figure 14. Vibration frequency response of the modeled transformer.

Table 5. Classification of the transformer modes based on mode shape type.

ID	Natural frequency (Hz)	Mode shape summary
Modes related to the transformer core (first five)	34	Symmetrical twist
	54	Asymmetrical deformation
	78	Asymmetrical deformation
	108	Asymmetrical bending
	205	Symmetrical bending
Modes related to the transformer windings (first five)	370	Axial and radial bending
	398	Cylindrical mode
	450	Axial displacement
	478	Twisting mode
	520	Radial bending
Modes related to the core and windings together (first three)	4	Out-of-plane deformation
	18	Out-of-plane deformation
	36	Out-of-plane bending

summarized in Table 5. In this table, mode shapes are divided into three types based on their participation in the vibration of the transformer structure: core-related modes, windings-related modes, and coupled modes. If the core vibrations contribute the most to the vibrations of the transformer structure, the vibration mode is classified as core-related. Winding-related modes have a similar definition. If both the winding and the core play significant roles, the mode distribution is said to be coupled. As shown in Table 5, the vibration modes of the core and the coupled modes are in the lower frequency range, while the vibration modes of the winding are often in the higher frequency range. In addition, in the frequency range above 1000 Hz, most of the vibrational resonance frequencies are related to single disks and winding assembly.

Since a quantitative understanding of the resonance of the transformer structure can benefit from mode shape analysis, representative mode shapes are provided for vibration resonances of the winding-related modes in Figure 15. This figure shows the vibration resonances of the first four mode shapes of the winding-related cases. Since most windings of practical transformers are cylindrical, the results obtained from the shape of the winding modes can also be useful for the winding-related modes of other power transformers. The first winding-related mode in Figure 15(a) is an axial and radial bending mode with both ends constrained, while the second winding-related mode is cylindrical. Most of the stress is applied to the upper part of the winding in these two modes. Based on these mode shapes, it can be concluded that the vibrations of the windings are most likely similar to a cylindrical shell. Excessive vibration in this situation produces buckling and deformations in the windings. As a result, the winding assembly cannot be regarded as a ring stack or a collection of lumped masses. In the case of other modes, as can be seen, the third mode is a combination of winding axial displacement and cylindrical modes. The fourth mode is a twisting mode that deforms the transformer winding in two directions simultaneously.

6.2. Transformer vibration modes under winding mechanical faults

The properties of transformer winding vibration modes in the presence of winding abnormalities are studied in this section. Based on the FEM analysis, differences in natural frequencies and the associated vibration energy distribution are demonstrated and discussed. In the presence of winding damage, the natural frequencies of the winding-related modes shift, as illustrated in Table 6. In all of the examined modes, the maximum deviations of the natural frequency are negative. The free buckling of the LV winding, on the other hand, raises the 3rd natural frequency by 9 Hz, suggesting that when the winding is damaged, the natural frequency shift is not necessarily negative or positive. In theory, using the modal displacement distribution as a monitoring indicator is straightforward. However, even when the transformer is offline, measuring winding modes is difficult. To use mode-shape-based monitoring techniques, the experimental approach and feasible online implementation must be improved.

As mentioned before, vibrations are transmitted through mechanical connections to the transformer tank. Therefore, when the windings are damaged, such as when winding buckling occurs, the vibration

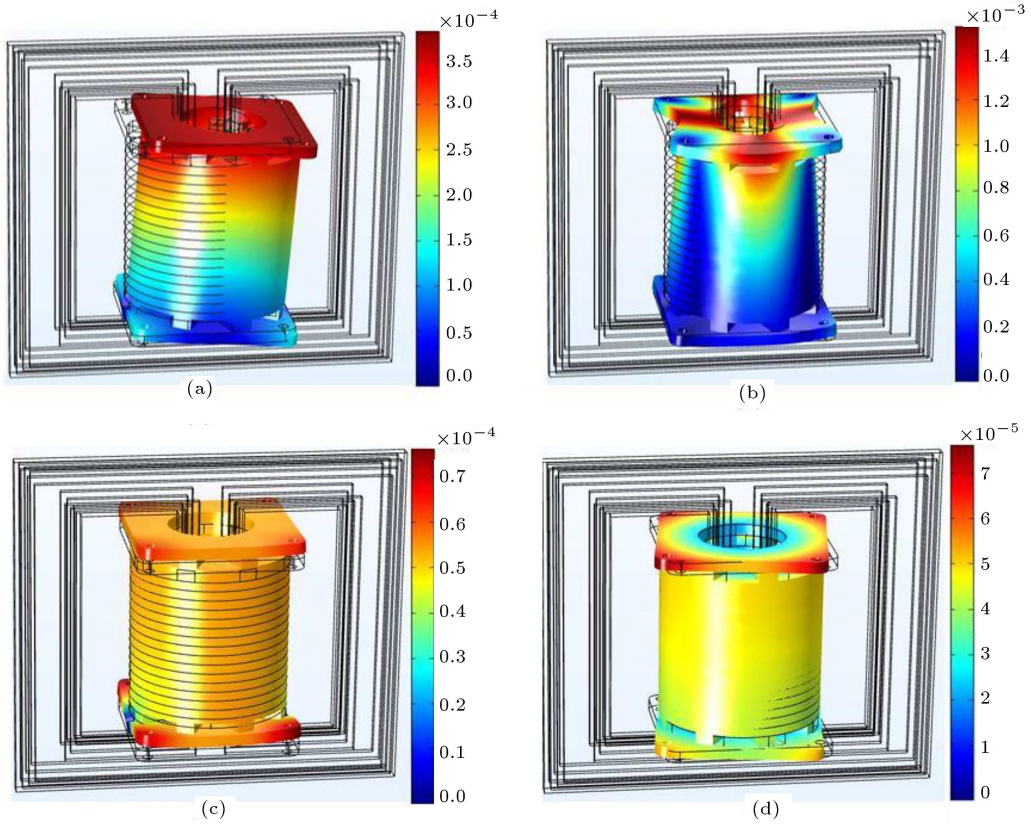

Figure 15. The first four winding-related modes at (a) 370 Hz, (b) 398 Hz, (c) 450 Hz, and (d) 478 Hz. The figure shows the displacement in mm.

Table 6. Changes in the natural frequencies of the winding-related modes under fault conditions.

Winding-related modes	Normal condition	LV free buckling	HV elongation	Winding twisting	Δf_{Max}
1	370	368.2	369.5	369	−1.8
2	398	391.6	396	398	−6.4
3	450	459	439	452.5	−11
4	478	469	463	480	−15

energy distribution of the winding changes, leading to a different vibration distribution of the transformer tank as a result of these connections. In other words, if several sensors are attached in different positions on the transformer tank, the amplitude ratio of their captured signals varies when a mechanical change is introduced in the winding. The vibration energy distribution of the tank is compared in Figure 16 for the healthy condition of the winding with mechanically damaged conditions on one of the tank faces. By comparing the vibration energy distribution of the tank in different states, several conclusions are drawn. Firstly, the amplitude of the vibration energy in the mechanical fault condition is significantly greater than that in the normal condition. It can also be seen from the energy distribution diagrams that the maximum energy density in mechanical fault modes, including winding buckling with an amplitude of 16 J/m^3, HV elongation with an amplitude of 9 J/m^3, and winding twisting with an amplitude of 12 J/m^3, is much larger than the amplitude of vibration energy in the normal state with an amplitude of 1.5 J/m^3. These characteristics can be used to characterize the mechanical condition of the winding. In addition, under normal winding conditions, the vibration energy distribution of the tank is symmetrical. In buckling and HV elongation fault conditions, the vibration energy is moved by specific patterns to the middle of the tank. In the winding twisting condition, the vibration energy is also distributed asymmetrically on the surface of the tank. Therefore, by monitoring the vibration energy distribution on the transformer tank, for example, using multiple sensors, it is possible to detect a mechanical variation in the transformer. The energy

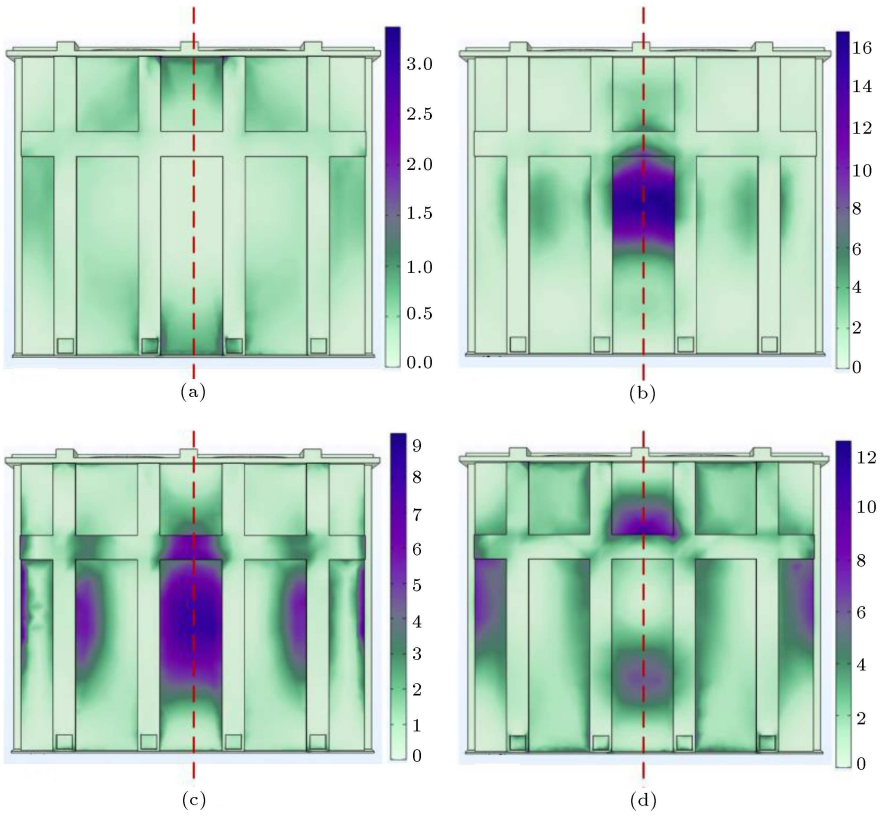

Figure 16. The vibration energy distribution (J/m^3) of the transformer tank in the (a) healthy condition; (b) LV free buckling; (c) HV elongation; and (d) winding twisting.

distribution patterns effectively allow for comparison of the energy distribution of vibration signals under different mechanical conditions.

7. Conclusions

Based on the vibration mechanism, this paper proposes a finite element model of transformer vibration stimulated by electromagnetic forces. The proposed model has been used to simulate the coupled field in transformers. This paper shows that mechanical changes in the active part influence mechanical oscillations both on the winding itself and on the transformer's tank wall. From the analysis of the vibrations measured from the tank surface, it is found that the signal amplitude recorded by sensors in different positions varies. Moreover, it is shown that in the case of a mechanical change in the winding, the harmonic contents of the captured vibration signal change, and this can be used as an indicator for transformer diagnosis. In the next section, the vibration modes of the winding are studied. Using the Finite Element Method (FEM) technique, the sections of the transformer involved in each resonance frequency and the related mode shapes can be determined. Furthermore, mechanical changes shift the resonance frequencies and vary the energy distribution of the vibration on the tank surface. Therefore, these two features can be used for further assessment of the transformer's mechanical situation. In summary, the finite element model offers possible methods for the vibration monitoring of a transformer. As the next step in future work, these observations need to be implemented in an experimental setup to prove their practicality in the field.

References

1. Secic, A., Krpan, M., and Kuzle, I. "Vibro-acoustic methods in the condition assessment of power transformers: A survey", *IEEE Access*, **7**, pp. 83915–83931 (2019). DOI: 10.1109/ACCESS.2019.2923809
2. Tran, Q.T., Davies, K., and Roose, L. "A review of health assessment techniques for distribution transformers", *Applied Sciences*, **10**(22), p. 8115 (2020). DOI: 10.3390/app10228115
3. Emara, M.M., Peppas, G.D., and Gonos I.F. "Two graphical shapes based on DGA for power transformer fault types discrimination", *IEEE Transactions on Dielectrics and Electrical Insulation*, **28**(3), pp. 981–987 (2021). DOI: 10.1109/TDEI.2021.009415
4. Gao, C., Yu, L., Xu, Y., et al. "Partial discharge localization inside transformer windings via fiber-optic acoustic sensor array", *IEEE Transactions on Power Delivery*, **34**(4), pp. 1251–1260 (2019). DOI: 10.1109/TPWRD.2018.2880230

5. Tenbohlen, S., Beltle, M., and Siegel, M. "PD monitoring of power transformers by UHF sensors", *International Symposium on Electrical Insulating Materials (ISEIM)*, Toyohashi, Japan, pp. 303–306 (2017). DOI: 10.23919/ISEIM.2017.8088747

6. Wang, H. and Butler, K.L. "Modeling transformer with internal winding faults by calculating leakage factors", *Proc. 31st North American Power Symposium (NAPS) Web-Based Computing for Power System Applications*, San Luis Obispo, USA, pp. 176–182 (1999).

7. Samimi, M.H., Tenbohlen, S., Akmal, A.A.S., et al. "Dismissing uncertainties in the FRA interpretation", *IEEE Transactions on Power Delivery*, **33**(4), pp. 2041–2043 (2018). DOI: 10.1109/TPWRD.2016.2618601

8. Samimi, M.H. and Dadashi Ilkhechi, H. "Survey of different sensors employed for the power transformer monitoring", *IET Science, Measurement & Technology*, **14**, pp. 1–8 (2020). DOI: 10.1049/iet-smt.2019.0103

9. Wang, Y., Zhang, J., Zhou, B., et al. "Magnetic shunt design and their effects on transformer winding electromagnetic forces", *Iranian Journal of Science and Technology, Transactions of Electrical Engineering*, **43**, pp. 97–105 (2019). DOI: 10.1007/s40998-018-0074-4

10. Geiβler, D. and Leibfried, T. "Short-circuit strength of power transformer windings-verification of tests by a finite element analysis-based model", *IEEE Transactions on Power Delivery*, **32**(4), pp. 1705–1712 (2017). DOI: 10.1109/TPWRD.2016.2572399

11. Wang, S., Wang, S., and Zhang, N. "Calculation and analysis of mechanical characteristics of transformer windings under short-circuit condition", *IEEE Transactions on Magnetics*, **55**(7), pp. 1–4 (2019). DOI: 10.1109/TMAG.2019.2898183

12. Murugan, R. and Ramasamy, R. "Understanding the power transformer component failures for health index-based maintenance planning in electric utilities", *Engineering Failure Analysis*, **96**, pp. 274–288 (2019). DOI: 10.1016/j.engfailanal.2018.10.011

13. Seyedshenava, S. and Ahmadpour, A. "Finite element method for optimal transformer connection based on induction motor characteristics analysis", *Ain Shams Engineering Journal*, **12**(2), pp. 1943–1957 (2021). DOI: 10.1016/j.asej.2020.12.008

14. Guo, J., Ma, X., and Ahmadpour, A. "Electrical-mechanical evaluation of the multi-cascaded induction motors under different conditions", *Energy*, **229**, p. 120664 (2021). DOI: 10.1016/j.energy.2021.120664

15. Kim, H., Chung, Y., Jin, J., et al. "Manifestation of flexural vibration modes of rails by the phase-based magnification method", *IEEE Access*, **9**, pp. 98121–98131 (2021).

16. Sarrafi, A., Mao, Z., Niezrecki, C., et al. "Vibration-based damage detection in wind turbine blades using Phase-based Motion Estimation and motion magnification", *Journal of Sound and Vibration*, **421**, pp. 300–318 (2018). DOI: 10.1016/j.jsv.2018.01.050

17. Civera, M., Zanotti Fragonara, L., and Surace, C. "An experimental study of the feasibility of phase-based video magnification for damage detection and localization in operational deflection shapes", *Strain*, **56**(2), p. e12336 (2020). DOI: 10.1111/str.12336

18. Report, A.C. "Bibliography on transformer noise", *IEEE Transactions on Power Apparatus and Systems*, **PAS-87**(2), pp. 372–387 (1968).

19. Fahnoe, H. "A study of sound levels of transformers", *Electrical Engineering*, **60**(6), pp. 277–282 (1941). DOI: 10.1109/EE.1941.6432149

20. Si, W., Yao, W., Guan, H., et al. "Numerical study of vibration characteristics for sensor membrane in transformer oil", *Energies*, **14**(6), p. 1662 (2021). DOI: 10.3390/en14061662

21. Foster, S.L. and Reiplinger, E. "Characteristics and control of transformer sound", *IEEE Transactions on Power Apparatus and Systems*, **PAS-100**, pp. 1072–1077 (1981). DOI: 10.1109/TPAS.1981.316573

22. Xu, L. and Liu, X. "Study on the three dimensions attenuated model and the algorithm of environmental noise in substations", *Proc. CSEE, Mathematics*, Dodoma, Tanzania, **32**, I0024 (2012).

23. Wu, G., Cheng, S.G., Huang, L., et al. "Prediction on the noise of 220 kV outdoor substation to environmental infection", *Noise and Vibration Control*, **27**, pp. 135–137 (2007).

24. Zhu, L., Yang, Q., Yan, R., et al. "Research on vibration and noise of power transformer cores including magnetostriction effects", *Transactions of China Electrotechnical Society*, **28**, pp. 1–6 (2013).

25. Hu, J., Liu, D., Liao, Q., et al. "Analysis of transformer electromagnetic vibration noise based on finite element method", *Transactions of China Electrotechnical Society*, **31**, pp. 81–88 (2016).

26. Ji, S., Li, Y., and Fu, C. "Application of on-load current method in monitoring the condition of transformer's core based on the vibration analysis method", *Proc. CSEE, Madrid, Spain*, **2**, pp. 154–158 (2003).

27. Yu, X., Li, Y., Jing, Y., et al. "Calculation and analysis of natural frequency of winding model of transformer", *Transformer*, **47**, pp. 5–8 (2010).

28. Bartoletti, C., Desiderio, M., Carlo, D.D., et al. "Vibro-acoustic techniques to diagnose power transformers", *IEEE Transactions on Power Delivery*, **19**(1), pp. 221–229 (2004).

29. Hong, K., Huang, H., and Zhou, J. "A method of real-time fault diagnosis for power transformers based on vibration analysis", *IET Measurement Science and Technology*, **26**, p. 115011 (2015). DOI: 10.1088/0957-0233/26/11/115011

30. Berler, Z., Golubev, A., Rusov, V., et al. "Vibro-acoustic method of transformer clamping pressure

monitoring", *Conference Record of the 2000 IEEE International Symposium on Electrical Insulation*, pp. 263–266 (2000). DOI: 10.1109/ELINSL.2000.845503

31. García, B., Burgos, J.C., and Alonso, Á.M. "Transformer tank vibration modeling as a method of detecting winding deformations-part I: theoretical foundation", *IEEE Transactions on Power Delivery*, **21**(1), pp. 157–163 (2005). DOI: 10.1109/TPWRD.2005.852280
32. García, B., Burgos, J.C., and Alonso, Á.M. "Transformer tank vibration modeling as a method of detecting winding deformations-part II: experimental verification", *IEEE Transactions on Power Delivery*, **21**(1), pp. 164–169 (2005). DOI: 10.1109/TPWRD.2005.852275
33. Ji, S., Luo, Y., and Li, Y. "Research on extraction technique of transformer core fundamental frequency vibration based on OLCM", *IEEE Transactions on Power Delivery*, **21**(4), pp. 1981–1988 (2006). DOI: 10.1109/TPWRD.2006.876665
34. Naranpanawe, L. and Ekanayake, C. "Finite element modelling of a transformer winding for vibration analysis", *2016 Australasian Universities Power Engineering Conference (AUPEC)*, Brisbane, QLD, Australia, pp. 1–6 (2016). DOI: 10.1109/AUPEC.2016.7749344
35. Qian, G., Lu, Y., Wang, F., et al. "Vibration response analysis of transformer winding by finite element method", *2016 IEEE/PES Transmission and Distribution Conference and Exposition (T&D)*, Dallas, TX, USA, pp. 1–5 (2016). DOI: 10.1109/TDC.2016.7519986
36. Jin, M. and Pan, J. "Vibration transmission from internal structures to the tank of an applied acoustics oil-filled power transformer", *Applied Acoustics*, **113**, pp. 1–6 (2016). DOI: 10.1016/j.apacoust.2016.05.022
37. Liu, M., Hubert, O., Mininger, X., et al. "Homogenized magnetoelastic behavior model for the computation of strain due to magnetostriction in transformers", *IEEE Transactions on Magnetics*, **52**(2), pp. 1–12 (2016). DOI: 10.1109/TMAG.2015.2493062
38. Beltle, M. and Tenbohlen, S. "Vibration analysis of power transformers", *18th International Symposium on High Voltage Engineering*, Seoul, Korea, pp. 1816–1821 (2013).
39. Rivas, E., Burgos, J.C., and Garcia-Prada, J.C. "Condition assessment of power OLTC by vibration analysis using wavelet transform", *IEEE Transactions on Power Delivery*, **24**(2), pp. 687–694 (2009). DOI: 10.1109/TPWRD.2009.2014268
40. Wang, Z., Zhang, Y., Zhang, D., et al. "Modeling of magnetostrictive property of electrical steel sheet under vectorial excitation", *IEEE Transactions on Magnetics*, **55**(6), pp. 1–4 (2019). DOI: 10.1109/TMAG.2019.2896892
41. Xiaomu, D., Tong, Z., and Jinxin, L. "Analysis of winding vibration characteristics of power transformers based on the finite-element method", *Energies*, **11**(9), 2404 (2018). DOI: 10.3390/en11092404
42. Wan, D.F. "Magnetic theory and its application", *Huazhong University of Science and Technology Press*, Wuhan, China, pp. 56–62 (1996).
43. Togun, N. and Bağdatli, S.M. "Nonlinear vibration of a nanobeam on a pasternak elastic foundation based on non-local euler-bernoulli beam theory", *Mathematical and Computational Applications*, **21**(1), p. 3 (2016). DOI: 10.3390/mca21010003
44. Hong, K., Huang, H., and Zhou, J. "Winding condition assessment of power transformers based on vibration correlation", *IEEE Transactions on Power Delivery*, **30**(4), pp. 1735–1742 (2015). DOI: 10.1109/TPWRD.2014.2376033
45. Zhang, F., Ji, S., Shi, Y., et al. "Investigation on the action of eddy current on tank vibration characteristics in dry-type transformer", *IEEE Transactions on Magnetics*, **55**(2), pp. 1–8 (2019). DOI: 10.1109/TMAG.2018.2883854
46. Wang, J., Gao, C., Duan, X., et al. "Multi-field coupling simulation and experimental study on transformer vibration caused by DC bias", *Journal of Electrical Engineering and Technology*, **10**(1), pp. 176–187 (2015). DOI: 10.5370/JEET.2015.10.1.176
47. Behjat, V., Shams, A., and Tamjidi, V. "Characterization of power transformer electromagnetic forces affected by winding faults", *Journal of Operation and Automation in Power Engineering*, **6**(1), pp. 40–49 (2018). DOI: 10.22098/joape.2018.2436.1210
48. Yan, T., Ren, C., Zhou, J., et al. "The study on vibration reduction of nonlinear time-delay dynamic absorber under external excitation", *Mathematical Problems in Engineering*, **2020**, pp. 1–11 (2020). DOI: 10.1155/2020/8578596
49. Shengchang, J., Lingyu, Z., and Yanming, L. "Study on transformer tank vibration characteristics in the field and its application", *Przeglad Elektrotechniczny*, **87**(2), pp. 205–211 (2011).
50. Beltle, M. and Tenbohlen, S. "Power transformer diagnosis based on mechanical oscillations due to AC and DC currents", *IEEE Transactions on Dielectrics and Electrical Insulation*, **23**(3), pp. 1515–1522 (2016). DOI: 10.1109/TDEI.2016.005537
51. Tavakoli, A., De Maria, L., Bartalesi, D., et al. "Diagnosis of transformers based on vibration data", *2019 IEEE 20th International Conference on Dielectric Liquids (ICDL)*, Roma, Italy, pp. 1–4 (2019). DOI: 10.1109/ICDL.2019.8796535
52. Leibfried, T. and Feser, K. "Monitoring of power transformers using the transfer function method", *IEEE Transactions on Power Delivery*, **14**(4), pp. 1333–1339 (1999). DOI: 10.1109/61.796226

Biographies

Amir Esmaeili Nezhad holds a Master's degree (GPA= 4/4) from the Faculty of Electrical and Computer Engineering at the University of Tehran, Iran.

His research interests include invasive and noninvasive methods for the condition assessment of power system equipment, focusing on transformers and on-load tap changers. Additionally, he has worked on power system optimization, power system flexibility, and the integration of renewable energy systems into power systems.

Mohammad Hamed Samimi received his PhD degree (Hons.) in Electrical Engineering from the University of Tehran, Tehran, Iran, in 2017. He carried out part of his PhD research at the University of Stuttgart, Stuttgart, Germany, under the DAAD scholarship award for the "bi-nationally supervised doctoral degree" program in 2015 and 2016. He has been associated with the High Voltage Institute of the University of Tehran as a Researcher and Assistant since 2009. He cooperated with the R&D Department of Nirou Trans Company, Shiraz, working as a consultant. He also worked for two years as a researcher in the power system protection office at the Iran Grid Management Company (IGMC), Tehran. In 2018, he joined the School of Electrical and Computer Engineering at the University of Tehran, where he currently serves as an Assistant Professor of Electrical Engineering. His research interests include the modeling, testing, condition monitoring, and diagnosis of high-voltage apparatuses.